Journal of Materials Chemistry B

Accepted Manuscript

ROYAL SOCIETY OF CHEMISTRY

www.rsc.org/materialsB

Journal of Materials Chemistry B RSCPublishing

ARTICLE

In vitro and in vivo evaluation of xanthan gum-succinic anhydride hydrogels for ionic strength-sensitive release of antibacterial agents

Cite this: DOI: 10.1039/xoxxoooooox

Received ooth January 2012,
Accepted ooth January 2012

DOI: 10.1039/xoxxoooooox

www.rsc.org/

Bailiang Wang[a, b]*, Yuemei Han[a], Quankui Lin[a, b], Huihua Liu[b], Chenghui Shen[b], Kaihui Nan[a,b], and Hao Chen[a, b]*

In this work, we report a new approach to prepare high gel performance hydrogels which are used as ionic strength-sensitive drug release system. Succinic anhydride (SA)–modified xanthan (XG–SA) derivatives were prepared and confirmed by Fourier transform-infrared spectroscopy and proton nuclear magnetic resonance spectroscopy. Rheological measurement showed storage moduli (G') and loss moduli (G") of XG-SA were much higher than native XG suggesting a higher stability of the hydrogels. XG-SA could form into stable hydrogels when the content of dry gel was 1.4 wt%. Drug release studies showed ionic strength-sensitive and sustained release of gentamicin (GS) for 9 days under aqueous physiological conditions. Biofilm inhibition assay revealed that the XG-SA/GS hydrogels were sufficient to inhibit the biofilm formation. Kirby-Bauer method showed that there was zone of inhibition around 8.2 mm indicating the excellent bactericidal function of the hydrogels. Cytocompatibility assessment against human lens epithelial cells revealed that the hydrogels supported cell adhesion, proliferation and migration when the loading dosage of GS was 1mg/g. The XG-SA/GS hydrogels were compared to native XG-SA in the rabbit subcutaneous *S. aureus* infection model. The XG-SA/GS hydrogels yielded a significantly lower degree of infection than XG-SA hydrogels at day 7. In this way, XG-SA hydrogels are promising drug delivery materials for antibacterial applications.

Introduction

The adherence of bacteria and subsequent formation of biofilm have been one of the most serious complications for many biomedical applications, causing device failure as well as tissue infections [1-3]. In the world, about 64% of the hospital acquired infections are caused by the adherence of pathogens on medical implants and devices [4]. Only in Europe, 5% of patients admitted to hospitals suffer from hospital-acquired infections leading to a mortality of 10% each year [5]. Once bacteria adhere on the surface of biomedical devices, bacteria multiply into colonies, secrete extracellular matrix and finally form biofilm which induce infection through releasing planktonic cells and toxins [6]. Biofilm formation is the second step in the biphasic bacterial attachment process. After the reversible attachment of bacteria within the first few hours the attachment becomes irreversible and a biofilm is formed [7]. Just owning to the formation of biofilm, antibacterial agents can hardly play its role and also generate drug resistant bacteria which can resist 1000-folds dose antibiotics in comparison with planktonic bacteria [8, 9]. Consequently, efficient treatment of bacterial infections should be local and immediate. Smart drug-delivery systems, which can locally and specifically release their antibacterial agents, have been developed to address the problems of bacterial attachment and colonization [10].

Hydrogels have found varied applications such as controlled drug release, cellular delivery, tissue engineering and as wound dressings due to the highly hydrated and three dimensional properties [11-13]. More importantly, hydrogels can swell in specific conditions by absorbing a large amount of water and de-swell by pushing out the absorbed water according to the environmental conditions such as temperature, pH, ionic strength, solvent polarity, etc [14, 15]. The suitability of hydrogels for the pharmaceutical applications is mainly determined by their mechanical properties, drug loading and controlled drug release capability. Antibacterial

wound dressings fabricated with silver nanoparticle incorporated hydrogels were also reported [16]. It is attractive to use a hydrogels nanofiber matrix to deliver therapeutic or antimicrobial agents due to its high surface area to volume ratio. Kuijpers et al. prepared chemically cross-linked gelatin chondroitin sulphate hydrogels which were evaluated as drug delivery systems for antibacterial proteins [17]. Silan et al. synthesized novel hydrogel particles based on poly(acrylonitrile) and prepared interpenetrating polymer network films with antibacterial properties which also can be used as drug delivery system [18]. In those cases, the use of a proper polymeric material may improve pharmacokinetic profiles of the encapsulated drug and prolong its efficacy. Particularly, local drug delivery systems exhibiting high initial release rate followed by a sustained release at an effective antibiotic concentration may allow control of infection while minimizing side effects and induced bacterial resistance [19-21].

Xanthan gum (XG) is an anionic, high molecular weight, exopolysaccharide produced by fermentation of sugars with the Gram-negative bacterium *Xanthomonas campestris*[22]. It is a heteropolysaccharide and the primary structure of XG consists of repeated pentasaccharide units formed by two glucose units, two mannose units, and one glucuronic acid unit[23]. It is non-toxic, hydrophilic and bidegradable bio-polymer which has been widely used in food, cosmetic and pharmaceutical industries[24-26]. The industrial applications of XG are based upon its exceptional rheological properties. In earlier studies graft copolymers of XG and vinyl monomer have been synthesized and evaluated as controlled release agent[24, 27, 28]. More importantly, XG hydrogels responds to external stimuli by exchanging intra- and inter-molecular interactions, causing a variety of polymer conformations. In solution the rigid helix–coil structure transforms into flexible coils whose stability and physical properties are strongly influenced by pH and the ionic environment[29-31]. XG is able to form physical or chemical gels, the physical ones being not as resistant as the chemical ones[32]. In order to form chemical gels XG was usually crosslinked with epichlorhydrin[33], but it is known that this crosslinking agent is toxic and carcinogenic[34]. For this reason, the exploring of new method to improve its rheological property and stability for biomedical implications is of great importance.

The number of carboxylic acid groups present on the carrier matrix play an important role for polyionic interaction with cationic protein drugs. Our goal was to develop hydrogels based on XG as carrier to load GS and sustained release of the drug. The drug loaded system need to first provide sufficient levels of antibiotics to eradicate an existing infection, prevent biofilm formation, and then are biocompatible with mammalian cells. In this work, XG were anionized to increase the carboxylic acid groups through succinylation. The rheological properties, gel performance as well as the drug loading and sustained release efficiency are investigated. The antibacterial properties both *in vitro* and *in vivo* are also discussed. This approach could represent a generalized strategy to prepare stimulative-responsibility hydrogels as drug loading system.

Materials and methods

Materials

Xanthan (viscosity: 25-70 mPa.s, 1% in H_2O, 25 °C), succinic anhydride (SA) and 4-dimethylaminopyridine (DMAP) were purchased from Sigma-Aldrich. *Staphylococcus aureus* (*S. aureus*, ATCC 6538) was kindly provided by Prof. Jian Ji (Zhejiang University, Hangzhou, China). Ultrapure distilled water was obtained after purification using a Millipore Milli-Q system (USA).

Synthesis of XG-SA

The method reported in the previous reports was used to prepare hydrogels based on XG[35-37]. The units of -COOH were introduced by reaction between the remaining -OH groups of the XG with SA. XG (3.0 g) was reacted with SA (1.5 g) in a reaction flask in the presence of 4-DMAP (0.15 g) as catalyst at room temperature. This mixture was reacted for 48 h under a stream of nitrogen gas. The resulting crude product was dialysed against milli-Q water (2.0 L) using dialysis bag (molecular weight cut-off 140,000) at 4 ºC. The purified XG-SA was finally freeze-dried.

In vitro release study

The release behavior of GS from XG-SA hydrogels was studied using a dialysis bag method. Briefly, 5 mL of 1 mg/mL GS solution was mixed with 0.07 g XG-SA dry gel to form into homogeneous hydrogels. The hydrogels were sealed in a dialysis bag and immersed in 50 mL of PBS (0.1 M, pH 7.4) at 37 °C for 216 h. At predetermined intervals, 0.3 mL aliquots of the release medium were withdrawn for quantitative determination of GS. GS concentrations were measured using a procedure described by Sampath and Robinson [38]. Briefly, an o-phthaldialdehyde reagent was made and stored for 24 h in a dark environment. The GS aliquot, o-phthaldialdehyde reagent, and isopropanol were mixed in equal proportions and stored for 30 min at room temperature. The ophthaldialdehyde reacted with the GS amino groups and chromophoric products were obtained, the absorbances of which were measured at 332 nm using a Genesys Spectronic 20 spectrophotometer (Spectronic Instruments, Rochester, NY). A calibration curve was used to calculate the GS concentrations in the samples.

Characterization of the XG-SA hydrogels

Rheological measurement was performed with a rheometer (DHR-3, TA Instruments, USA). Hydrogel samples were prepared from 1.4 wt% XG-SA hydrogels loading 1 mg/mL GS. The hydrogels were placed on a parallel-plate of 40 mm diameter with a gap of 31 mm for measurement. Rheological test parameters, storage

moduli (G') and loss moduli (G") were monitored as a function of frequency at room temperature. All rheological studies were performed in triplicate and results were expressed as mean value ± S.D.

Proton Nuclear Magnetic Resonance (^{1}H NMR) was measured with a Bruker 400 NMR spectrometer at 25 ^{o}C, using deuteroxide (D_2O) as solvent. Fourier transforms infrared spectroscopy (FT-IR) were measured on a FT-IR spectrometry (Bruker Optics). The samples were prepared as KBr disk.

In vitro antibacterial test

Antimicrobial tests of hydrogels were conducted qualitatively and quantitatively by the zone inhibition test and bacterial LIVE/DEAD staining methods respectively with *S. aureus* as model bacteria. Zone inhibition test was carried out with a modified agar diffusion assay. GS-loaded XG-SA hydrogels were placed on nutrient agar in Petri dishes which had been seeded with 0.2 mL of 1.0×10^6 cells/mL bacteria suspension. The Petri dishes were examined for zone of inhibition after 24 h incubation at 37 ºC. The area clearing surrounded the film where bacteria were not capable of growing was reported as the zone of inhibition. A LIVE/DEAD BacLight bacterial viability kit (L-7012, Invitrogen) was used to determine bacterial cell viability. This test evaluates the structural integrity of bacterial membrane. The GS-loaded XG-SA hydrogels and native XG-SA hydrogels were incubated with 10 mL 1.0×10^5 cells/mL *S. aureus* suspensions in PBS for 24 h and stained according to the kit protocol. After careful washing, the samples were sealed with tin foil and observed by fluorescence microscope investigation (Zeiss, Germany).

Cytotoxicity assays

Cell cultivation

The human lens epithelial cells (HLECs, from ATCC, SRA01/04) were grown in DMEM/F12 (1:1) mixed medium supplemented with 10 % fetal bovine serum, 100 U/mL penicillin, and 100 μg/mL streptomycin in a 5 % CO_2 incubator at 37 ºC. Confluent cells were digested using 0.25 % trypsin-0.02 % EDTA, followed by centrifugation (1000 g for 3 min) to harvest the cells. Subsequently, the single cell suspension was used for cell number calculation using haemacytometer. After confluence, cells were digested and resuspended for cultivation on the materials. The HLECs were seeded onto the specimens at a density of 1.0×10^4 cells per sample by using 96-well tissue culture plate as the holder, cultivation was conducted for 24 h. Then, FDA and CCK-8 were used for the viability and morphology studies of cells grown on the resulting coatings.

Cell viability

CCK-8 (Beyotime, China) assay was employed in this experiment to quantitatively evaluate the cell viability. After HLECs were inoculated on the hydrogels for 24 h, the original medium was replaced by 100 μL 10 % FBS DMEM/F12 (1:1) mixed medium contains 10 μL CCK-8. It was incubated at 37 °C for 2 h to form water dissoluble formazan. Then 100 μL of the above formazan solution were taken from each sample and added to one well of a 96-well plate, six parallel replicates were prepared. The absorbance at 450 nm (calibrated wave) was determined using a microplate reader (Multiskan MK33, Thermo electron corporation, China). Tissue culture plates (TCPS) without any coating were used as a control.

Cell morphology

FDA (Sigma) is an indicator of membrane integrity and cytoplasmic esterase activity. The cell monolayers on different surfaces were stained with FDA for fluorescence microscope investigation (Zeiss, Germany) at 10× magnification in fluorescein filter, 488 nm excitation. Stock solutions were prepared by dissolving 5.0 mg/mL FDA in acetone. The working solution was freshly prepared by adding 5.0 μL of FDA stock solution into 5.0 mL of PBS. FDA solution (20 μL) was added into each well of a 96-well plate and incubated for 5 min. The hydrogels were then washed twice with PBS and placed on a glass slide for fluorescence microscope examination. The 488 nm wavelength of the laser was used to excite the dye. Cells incubated into wells that did not contain hydrogels were used as controls.

Animal experiments of antibacterial activity

The approval of the local laboratory animal committee (Laboratory Animal Ethics Committee of Wenzhou Medical University) for this study was obtained. Experiments were carried out in New Zealand White rabbits, weighing between 2.5 and 3.5 kg (obtained from Animal Administration Center of Wenzhou Medical University). The rabbits were treated in accordance with guidelines set forth by the Association for Research in Vision and Ophthalmology. Two groups of animals were studied for GS-loaded XG-SA hydrogels and unloaded hydrogels, respectively. All implants were sterilized prior to implantation and stored in sealed petri dishes.

The animal model used conforms to that described by Hansen[39]. New Zealand White rabbits were anesthetized using isoflorane delivered by facemask. A broad area of the back was shaved, and the underlying skin washed with surgical scrub, wiped with alcohol, painted with betadine, and draped for surgery. Under sterile conditions, two subcutaneous symmetrical GS-loaded XG-SA hydrogels and unloaded hydrogels implants were created on either side of the spine; care was taken to ensure broad physical separation between the implants to eliminate cross-contamination risks. In the

rabbits, the subcutaneous pocket was then inoculated with 10 mL of the 10^8 cells/mL *S. aureus* suspension. The incisions were closed in a single layer with 4-0 interrupted nylon suture and the epidermis was cleaned with 2 % H_2O_2. Rats were housed individually and given ad libitum access to food and water.

Animals were then observed daily throughout a 1 week period, after which they were returned to the operating room and prepared as above. Each pocket was opened via a small incision distinct from the prior wound, through which two sterile cotton swabs were inserted, sequentially. Animals were then euthanized, and the incision extended. A closed container containing the implant immersed in 5 mL of solution was vigorously vortexed for 30 s, followed by sonication for 5 min. From the solution, 0.2 mL was plated onto the triplicate solid agar using the spread plate method. After incubating for 24 h, the number of viable bacteria was counted and the results were expressed as mean colony forming units (CFU) per mL. After obtaining culture samples, each pocket was excised en bloc, and transmural sections from representative areas taken. Specimens were fixed in 10% formalin and embedded in paraffin blocks. Tissue sections, 5 mm thick, were mounted onto slides, which were stained using Hematoxylin and Eosin.

Statistical analysis

All experiments were conducted in triplicate, and data points were expressed as the mean. Two sample t test in origin 8.0 (Microcal, USA) were used to compare data obtained with the different samples under identical treatments. A value of $p < 0.05$ was considered significant.

Results and discussion

Development of XG-SA hydrogels

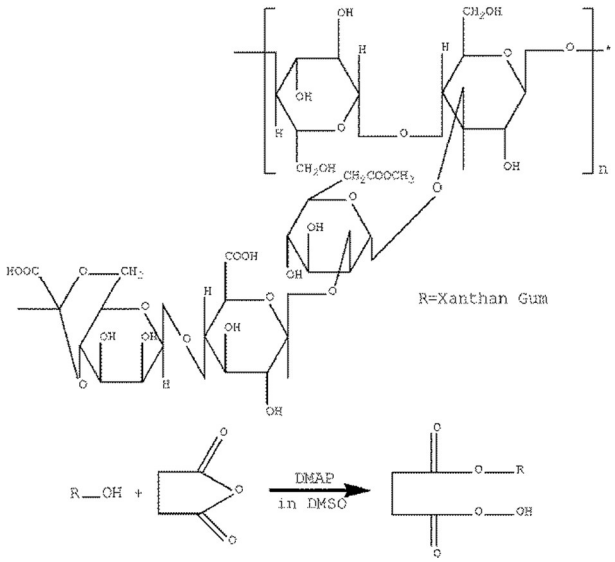

Fig. 1. Molecular formula of XG and succinylation of XG with SA to form XG-SA.

Immobilization and sustained release of antimicrobial molecules from biomedical surfaces is an efficient approach to prevent biomedical infections. The development of improved drug release systems is dependent on the selection of an appropriate carrier capable of controlling the delivery. Responsive polymers, in particular hydrophilic natural carbohydrate polymers, are the promising new versatile carriers for the preparation of controlled release systems. XG offers a potential utility as a drug carrier because of its inertness and biocompatibility. XG has the potential advantage of drug release with zero order release kinetics and the drug release is influenced by the pH and the presence of ions in the medium. To develop XG as a drug carrier, succinoylation of XG represented one of the most versatile transformations as it provided XG access to a variety of valuable properties. As shown in Fig.1, after succinoylation, the modified XG made carboxyl acid groups introduced via an ester linkage, which made XG a good drug carrier. As depicted in Fig. 2, it was clearly observed that the system turned into unflowable hydrogels at a very low contains (1.4 wt%), while the unmodified XG was flowable fluid at such concentration.

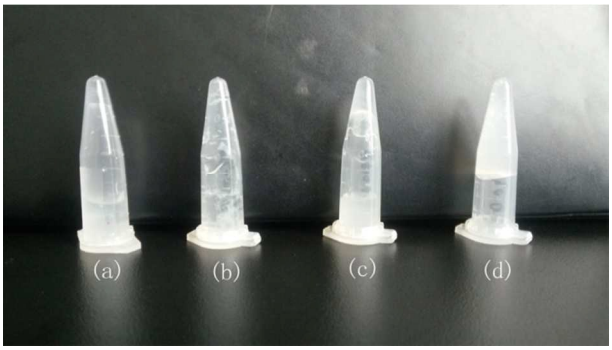

Fig. 2. The apparent gel-forming properties of (a) 1.4 wt% XG, (b) 0.35 wt % XG-SA, (c) 0.7 wt % XG-SA and (d) 1.4 wt % XG-SA in water.

Characterization of XG-SA

FT-IR measurement

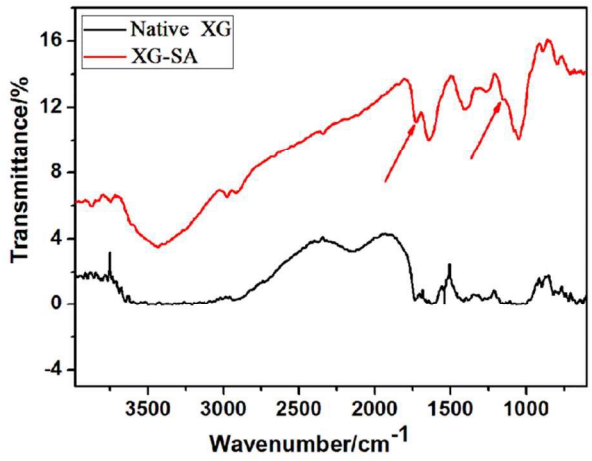

Fig. 3. FT-IR spectra of native XG and XG-SA. FTIR spectra of XG and XG-SA were recorded to study the modification of the XG and were presented in Fig. 3. The spectra of XG and XG-SA both displayed the typical profile of polysaccharides in the range 920-1100 cm^{-1} (characteristic peaks attributed to CO/CC bond stretching). The peaks at 1028-1084 cm^{-1} were characteristic of the anhydroglucose ring. The peak at 1408 cm^{-1} was due to OH bending[27]. Compared with the spectrum of XG, the spectrum of XG-SA provided characteristics absorption bands at 1728 cm^{-1} and 1154 cm^{-1}. The former band at 1728 cm^{-1} was indicative of absorption by carbonyl groups in carboxyl acids and esters. According to the previous reports, the absorption by carbonyl bond in esters and carboxylic acids often gave characteristic peaks at about 1750 cm^{-1} and 1710 cm^{-1} which were strongly overlapped and resulted in the peak at 1728 cm^{-1}. The new peak at 1154 cm^{-1} is due to the C-O and C-O-C stretching[40, 41]. These results indicated that the succinoylated XG was synthesized in this study.

^{1}H NMR measurement

The ^{1}H NMR has been used extensively qualitatively and quantitatively to determine the amount of SA groups attached to XG. Fig. 4 showed the typical ^{1}H NMR spectrum of XG-SA samples. Evident peak observed at 4.79 ppm was due to deutriated water used for sample preparation. The two peaks at 1.3 and 2.2 ppm correspond to acetate and pyruvate groups of the polymer. Peaks found between 3.2 and 3.9 ppm correspond to carbon linked to hydroxyl group and glucoronic acid, respectively. Peaks found between 4.4 and 4.7 ppm correspond to protons of β carbon of pyranose. Peaks found between 2.5 and 2.7 ppm corresponded to -CH_2-CH_2- of succinyl groups, which demonstrated the presence of SA. Furthermore, the degree of succinoylation was determined. When the XG/SA ratio was 2:1, the degree of succinoylation value of XG-SA was 0.18.

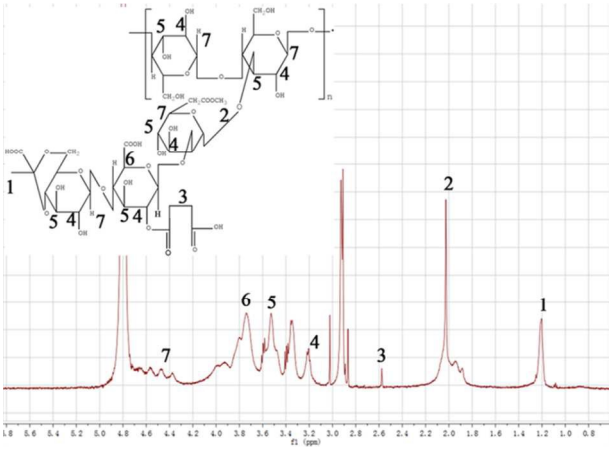

Fig. 4. ^{1}H-NMR spectrum of XG-SA.

Rheological measurements

Fig. 5 showed the mechanical spectra of XG and XG-SA after the preparation of the hydrogels at 25 °C. In case of native XG, the network formation was mainly caused by physical entanglements, because G' was almost equal to G". By succinoylation of XG with SA, the formation of secondary bonds was promoted: G' became larger than G" suggesting that the system was more elastic than viscous. And the length of the linear viscoelastic region increased and both moduli became less dependent on frequency. The XG-SA matrices behaved as strong gels with storage moduli higher than 1 000 Pa and without variations in all explored range of frequencies. Also the loss moduli, with values of the order of 100 Pa, did not show any dependence on the frequency, as expected for a three-dimensional network. By introducing of SA onto XG, the charge screening the intra- and intermolecular attraction between the polymer segments was greater than the segment-water affinity and the XG chain would tend to coil up or adopt a more rigid structure (increasing G'). The elastic property of XG-SA hydrogels were expected to maintain its integrity and helped to prevent drug loss

from blinking, yet resulting in the prolonged residence time of the drug from the matrix.

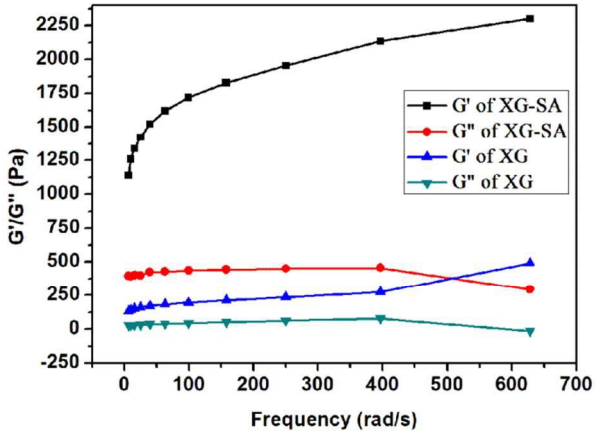

Fig. 5. Rheological property of native XG and XG-SA hydrogels as a function of frequency.

In vitro release studies

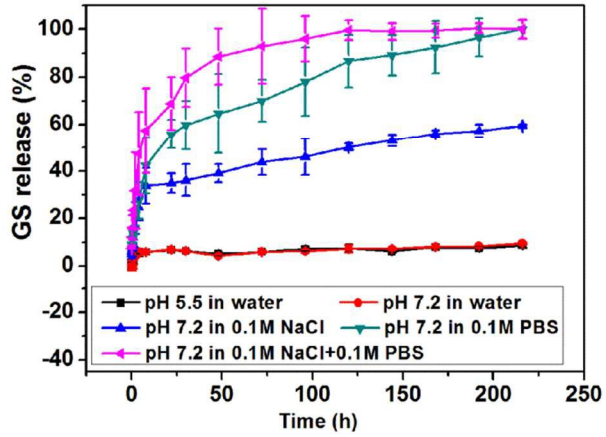

Fig. 6. Normalized cumulative GS release from the XG-SA/GS hydrogels.

In studying the effects of pH and ionic strength on the drug release kinetics profiles, the GS-loaded XG-SA hydrogels were immersed in the water with pH 5.5, 7.2, in 0.1 M PBS, 0.1 M NaCl and in 0.1 M PBS+0.1 M NaCl with pH at 7.2 for examining. The ability of XG-SA as sustained release materials was evaluated in vitro by conducting studies for 216 h. The percentage of GS released from hydrogels was plotted as a function with time. As shown in Fig. 6, under pH 5.5 and 7.2 in water, the total amount of GS released was about the same and was about 5% of the total GS in the matrix. The differences of release profiles were probably due to the hydration behavior and the (inter- and intra-) molecular interactions of the hydrophilic polymers in the matrices[42]. The strong synergistic interactions between polymers leaded to the formation of tight network to retard the dissolved drug. The high degree of gum hydration with simultaneous swelling resulted in the lengthening of the drug diffusion pathway and the reduction of drug release rate.

However, the rate of release increased significantly as the ionic strength of the surrounding environment increased. The hydrogels were immersed in PBS with different NaCl concentration, an ionic buffer that closely models conditions of the human body fluid without the biological components, maintained at 37 °C in a water bath. The XG-SA/GS hydrogels completed 35 %, 55 % and 69% of its release of the total GS within 24 h after being immersed in 0.1 M NaCl, 0.1 M PBS and 0.1 M PBS+0.1 M NaCl solutions respectively, displayed initial rapid release of the drug. Furthermore, the hydrogels completed 56% and 100 % release within 216 h in NaCl solution and PBS buffer respectively, which clearly indicated the sustained release process of GS. As a consequence, it is useful to use ionic strength as trigger for controlled release of GS from the matrices. GS was soluble in the pH range tested and diffused into the hydrogels and bound to the free carboxylate groups. The release of GS from the hydrogel matrix was dependent on the swelling and the dissolution/erosion of the matrix.

During the initial rapid 24 h, the fast release in buffered solutions over nonbuffered solutions was caused by the higher ionic concentration within the buffered solutions. The ions that were present in the buffered environment would shield the charges within the hydrogels, weakening the electrostatic interactions that held the hydrogels together. Consequently, the hydrogels swelled to a greater degree than under nonbuffered conditions. This allowed for rapid diffusion of GS throughout the bulk of the matrices. During the dissolution period 24-216 h, the drug release rate for all the formulations was nearly constant, implying the synchronization between swelling and erosion of the polymer in maintaining a constant gel layer. These results indicated that higher initial release would be effective to combat the microorganisms already present in the contaminated wound while a further slow and sustained release would suppress any new infections.

Antibacterial property of the GS-loaded hydrogels

Zone of inhibition (ZOI) assays

To evaluate the anti-adhesion and bactericidal efficiency of the GS-loaded hydrogels, Kirby-Bauer and Bacterial LIVE/DEAD staining methods were used using *S. aureus* as model bacteria. As indicated in Fig. 7a, no zone of inhibition was observed in the culture plates containing XG-SA hydrogels unloaded GS which was expected in these blank samples. This confirmed that neither XG nor the SA inhibited the growth of bacteria. However, the hydrogels containing GS showed zones of inhibition about 8.2 mm indicating the excellent bactericidal function. Even after 48 h and 120 h sustained release of GS from the matrices, there were also zones of inhibition about 7.5 mm and 6.3 mm respectively (Fig. 7c and 7d). Therefore, it indicated the effectiveness of incorporation and sustained release of drug from the XG-SA hydrogels.

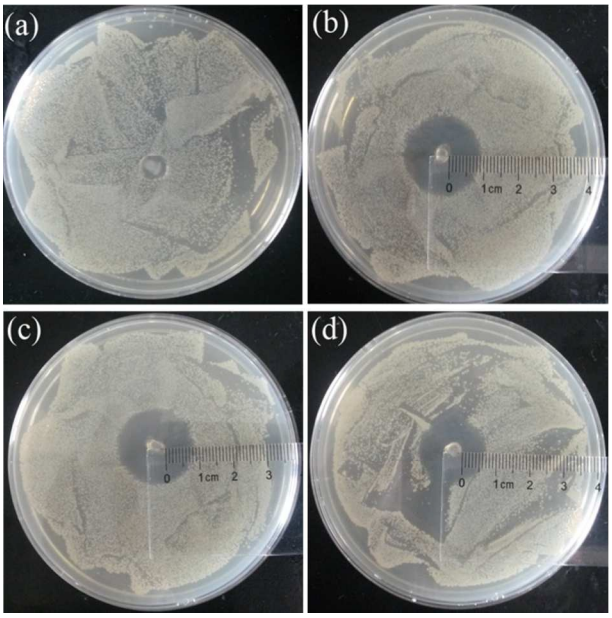

Fig. 7. Inhibition zones of (a) native XG-SA, (b) XG-SA/GS hydrogels before release and GS-loaded XG-SA hydrogels after being immersed in PBS for (c) 48 h and (d) 120 h against *S. aureus.*

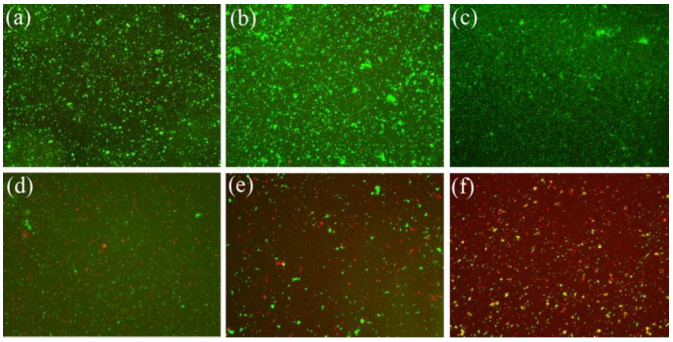

Fig. 8. Fluorescent microscopy images of *S. aureus* adhesions on XG-SA hydrogels at: (a) 4 h, (b) 24 h and (c) 72 h and on GS-loaded XG-SA hydrogels at (d) 4 h, (e) 24 h and (e) 72 h (the magnification was 10×).

Bacterial LIVE/DEAD staining methods

To quantify the distribution of viable (green fluorescence) and dead (red fluorescence) bacteria on the hydrogels, a LIVE/DEAD BacLight bacterial viability kit was used to stain the bacteria after incubation for 4 h, 24 h and 72 h respectively. As shown in Fig. 8, the surfaces of the native and GS-loaded XG-SA hydrogels were observed by staining with a combination dye of SYTO 9 and PI. There were numerous readily distinguishable bacterial cells with green fluorescence, either individually or in small clusters, were distributed on the native XG-SA surface after immersion in the *S. aureus* suspension (Fig. 8a, 8b and 8c). Meanwhile, a much lower number of bacteria cells detected on the surface of GS-loaded XG-SA which implied the effective antimicrobial activities of the hydrogels against *S. aureus* (Fig. 8d, 8e and 8f). It could be due to the rapid release of GS into the bacteria solution and fast killing of the bacteria. Also the hydrogels took up large quantities of free water, which built up a stable defence layer to resist bacterial adhesion [2].

On the surface of native XG-SA hydrogels, most of *S. aureus* remained intact as shown by the large number of green cells after 4 h of incubation. As for the GS-loaded hydrogels, there was a certain degree of killing of *S. aureus* although it failed to kill the majority of bacteria (around 50% of bacteria killed). After 24 h incubation with *S. aureus*, the number of bacterial cells increased greatly on the native XG-SA hydrogels. In sharp contrast, much less bacterial cells were found on the GS-loaded hydrogels surface although some bacterial clusters were seen. It clearly suggested that the anti-adhesion and antimicrobial activity of the hydrogels could be preserved for an extended period of time. Upon prolonging the exposure time to 72 h, the bacterial clusters with green fluorescence grew denser and aggregated to an initial form of a biofilm on native XG-SA hydrogels (Fig. 8c). On the other hand, around 90% of *S. aureus* were found dead and only 10% of cells remained intact on the GS-loaded hydrogels surface. The result supported that the XG-SA hydrogels prolonged releasing antibiotics possessed significant antimicrobial properties against bacteria.

Cell viability assays

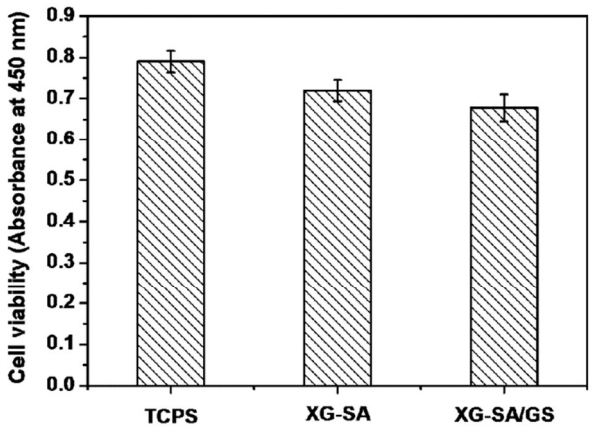

Fig. 9. The cell viability assay of HLECs cultured on the surfaces of (a) TCPS, (b) XG-SA hydrogels, (c) GS-loaded XG-SA hydrogels for 24 h. The absorbance of the diluted Cell Counting Kit solution has been deducted from each data point and the statistical significance is indicated by different letters ($p < 0.05$).

The interaction of cells with their surrounding environment is critical to determine the ultimate functionality of the implanted devices. Cell adhesion is the first cellular event during cell-implant interactions, which is a critical factor determining the clinical success of an implant[43]. HLECs were used to test the cytotoxicity by cell morphology and activity evaluation with TCPS as negative controls. As depicted in Fig. 9, HLECs activity on the native XG-SA showed more or less the same as that on TCPS (91.1%). Moreover, the cell viability of the HLECs on the GS-loaded hydrogels was not

very low (85.8% of that on TCPS), which showed low cytotoxicity toward HLECs. To illustrate the growth behaviour of HLECs on various surfaces, morphology and density of HLECs after growth for 24 h and FDA staining were studied. As shown in Fig. 10a, the surface of TCPS was good for HLECs growth and proliferation. On the other hand, the cell density on native and GS-loaded XG-SA hydrogels was less than that on TCPS. However, the cells maintained normal spreading morphology which indicated good cellular biocompatibility of the hydrogels.

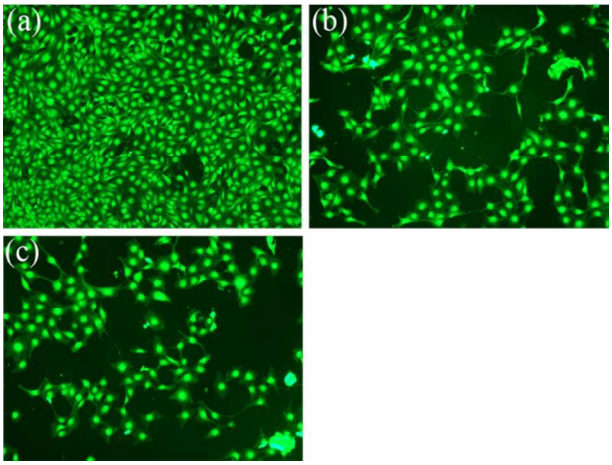

Fig. 10. Growth and morphology of HLECs stained with FDA after 24 h of incubation on (a) TCPS, (b) XG-SA hydrogels, (c) GS-loaded XG-SA hydrogels under fluorescence microscopy (the magnification was 10×).

In vivo antibacterial activity of the XG-SA/GS hydrogels

Because *S. aureus* a gram positive bacterial strain causes 65% human pathogenic diseases, as it is a common cause of skin infections, respiratory disease, and chronic osteomyelitis. Therefore, the materials were evaluated *in vivo* in a rabbit model in which hydrogels were inoculated with 10 mL of the 10^8 cells/mL *S. aureus* strain and examined. There were 24 rabbits in total with twelve animals each for the XG-SA/GS hydrogels and native XG-SA for the seven days observation period. Photographs of the tested samples are shown in Fig. 11. At day 7, it could be seen that no erythema or edema was observed in any of the GS release samples during the testing. On the country, the surgical sites implanted with native XG-SA showed significant redness and edema indicating severe inflammatory reaction. Also there was elevated bump which was relatively bigger than that of implanted with GS loaded hydrogels (Fig. 11b and 11e). Then the wound was cut to examine the inflammatory responses of the surrounding tissue to the materials. As for the XG-SA hydrogels, significant amounts of purulence were found in all bacterially challenged surgical sites, which indicated severe infection (Fig. 11c). In contrast, a significantly lower infection rate was observed for XG-SA/GS hydrogels that sustained released GS. Two of the twelve eluent (16.7 %) tested positive for viable *S. aureus* with minor infection. The sustained-release of GS from the XG-SA hydrogels could efficiently prevent bacterial infections and reduce inflammations toward implants.

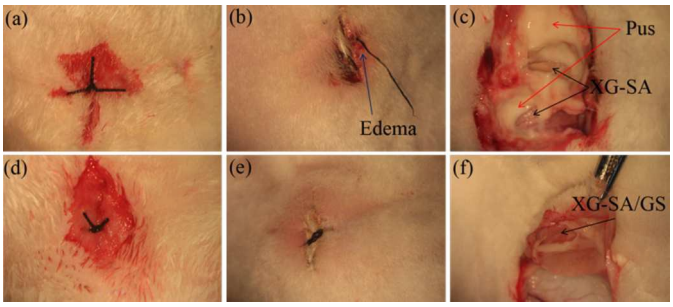

Fig. 11. Photographs of pockets implanted with native XG-SA hydrogels: (a) after operation, (b) at day 7, (c) opened at day 7 and pockets implanted with GS-loaded XG-SA hydrogels: (d) after operation, (e) at day 7 and (f) opened at day 7.

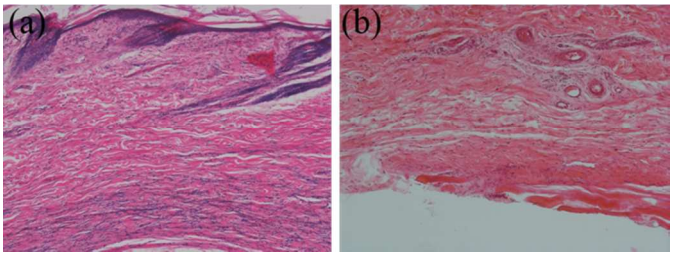

Fig. 12. Images of hematoxylin and eosin stained sections of surrounding connective tissues of (a) native XG-SA hydrogels and (b) GS-loaded XG-SA hydrogels.

Fig.12 showed the tissue slice diagram of the tissues adhering to the implants stained by HE stain at day 7 after implantation. For different samples, fewer inflammatory cells appeared in the XG-SA/GS hydrogels implant group than other group, indicating that GS loading and release played an important anti-inflammatory role (Fig. 12b). The wound that implanted with native XG-SA hydrogels was dominated by acute inflammatory response, which was surrounded by a relatively thick layer of chronic active inflammation and necrosis (Fig. 12a). The number of multinucleated giant cells showed statistically significant differences between two kinds of implants. These results demonstrated the high local release of GS from the XG-SA hydrogels might be an advantage compared to hydrogels without GS loading in preventing infections and inflammations.

Conclusions

In this article, the XG-SA was firstly synthesized through succinylation of XG with SA to increase the carboxyl groups and enhance gel performance. Rheological measurements indicated that XG-SA system was more elastic than XG and tended to adopt a more rigid structure. The prolonged release of GS showed ionic strength-sensitive and could last 9 days. The drug loading hydrogels were demonstrated efficacious against *S. aureus* and nontoxic toward HLECs. The XG-SA/GS hydrogels yielded a significantly

lower degree of infection than native XG-SA hydrogels in an *in vivo* rabbit subcutaneous *S. aureus* infection model at day 7. This approach represents a generalized strategy for incorporating charged small molecules into hydrogels, which can be used to modify implant and other biomedical devices.

Acknowledgements

National Natural Science Foundation of China (51403158, 81271703, 31570959), the International Scientific &Technological Cooperation Projects (2012DFB30020), Natural Science Foundation of Zhejiang Province (LY12H12005) and Science & Technology Program of Wenzhou (S20140005) are greatly acknowledged.

Notes and references

[a]School of Ophthalmology & Optometry, Eye Hospital, Wenzhou Medical University, Wenzhou, 325027, China

[b]Wenzhou Institute of Biomaterials and Engineering, Chinese Academy of Sciences, Wenzhou, 32500, China

* Corresponding author. Fax: +86 577 88067962.

E-mail:wangbailiang2006@aliyun.com (B.L. Wang),

Chenhao823@mail.eye.ac.cn (H. Chen).

† Footnotes should appear here. These might include comments relevant to but not central to the matter under discussion, limited experimental and spectral data, and crystallographic data.

Electronic Supplementary Information (ESI) available: [details of any supplementary information available should be included here]. See DOI: 10.1039/b000000x/

1. Y. K. Jo, J. H. Seo, B.-H. Choi, B. J. Kim, H. H. Shin, B. H. Hwang and H. J. Cha, *Acs Applied Materials & Interfaces*, 2014, **6**, 20242-20253.
2. J. H. Fu, J. Ji, W. Y. Yuan and J. C. Shen, *Biomaterials*, 2005, **26**, 6684-6692.
3. B. L. Wang, T. W. Jin, Y. M. Han, C. H. Shen, Q. Li, Q. K. Lin and H. Chen, *Journal of Materials Chemistry B*, 2015, **3**, 5501-5510.
4. B.-l. Wang, K.-f. Ren, H. C. J.-l. Wang and J. Ji, *Acs Applied Materials & Interfaces*, 2013, **5**, 4136-4143.
5. J. A. Lichter, M. T. Thompson, M. Delgadillo, T. Nishikawa, M. F. Rubner and K. J. Van Vliet, *Biomacromolecules*, 2008, **9**, 1571-1578.
6. B. L. Wang, X. S. Liu, Y. Ji, K. F. Ren and J. Ji, *Carbohydrate Polymers*, 2012, **90**, 8-15.
7. J. A. Lichter, K. J. Van Vliet and M. F. Rubner, *Macromolecules*, 2009, **42**, 8573-8586.
8. B. L. Wang, Q. K. Lin, T. W. Jin, C. H. Shen, J. M. Tang, Y. M. Hana and H. Chen, *Rsc Advances*, 2015, **5**, 3597-3604.
9. E. M. Anderson, M. L. Noble, S. Garty, H. Y. Ma, J. D. Bryers, T. T. Shen and B. D. Ratner, *Biomaterials*, 2009, **30**, 5675-5681.
10. S. Wong, M. S. Shim and Y. J. Kwon, *Journal of Materials Chemistry B*, 2014, **2**, 595-615.
11. M. M. Babic, K. M. Antic, J. S. J. Vukovic, B. D. Bozic, S. Z. Davidovic, J. M. Filipovic and S. L. Tomic, *Journal of Materials Science*, 2015, **50**, 906-922.
12. A. L. Z. Lee, V. W. L. Ng, G. L. Poon, X. Y. Ke, J. L. Hedrick and Y. Y. Yang, *Advanced Healthcare Materials*, 2015, **4**.
13. M. A. Lungan, M. Popa, S. Racovita, G. Hitruc, F. Doroftei, J. Desbrieres and S. Vasiliu, *Carbohydrate Polymers*, 2015, **125**, 323-333.
14. K. Malzahn, W. D. Jamieson, M. Droge, V. Mailander, A. T. A. Jenkins, C. K. Weiss and K. Landfester, *Journal of Materials Chemistry B*, 2014, **2**, 2175-2183.
15. X. Y. Gao, Y. Cao, X. F. Song, Z. Zhang, X. L. Zhuang, C. L. He and X. S. Chen, *Macromolecular Bioscience*, 2014, **14**, 565-575.
16. V. Rattanaruengsrikul, N. Pimpha and P. Supaphol, *Journal of Applied Polymer Science*, 2012, **124**, 1668-1682.
17. A. J. Kuijpers, P. B. van Wachem, M. J. A. van Luyn, L. A. Brouwer, G. H. M. Engbers, J. Krijgsveld, S. A. J. Zaat, J. Dankert and J. Feijin, *Biomaterials*, 2000, **21**, 1763-1772.
18. C. Silan, A. Akcali, M. T. Otkun, N. Ozbey, S. Butun, O. Ozay and N. Sahiner, *Colloids and Surfaces B-Biointerfaces*, 2012, **89**, 248-253.
19. F. De Cicco, A. Porta, F. Sansone, R. P. Aquino and P. Del Gaudio, *International Journal of Pharmaceutics*, 2014, **473**, 30-37.
20. M. Aviv, I. Berdicevsky and M. Zilberman, *Journal of Biomedical Materials Research Part A*, 2007, **83a**, 10-19.
21. G. R. Persson, G. E. Salvi, L. J. A. Heitz-Mayfield and N. P. Lang, *Clin Oral Implan Res*, 2006, **17**, 386-393.
22. Y. C. You, L. Y. Dong, K. Dong, W. Xu, Y. Yan, L. Zhang, K. Wang and F. J. Xing, *Carbohydrate Polymers*, 2015, **130**, 243-253.
23. R. R. Shiledar, A. A. Tagalpallewar and C. R. Kokare, *Carbohydrate Polymers*, 2014, **101**, 1234-1242.
24. F. Anjum, S. A. Bukhari, M. Siddique, M. Shahid, J. H. Potgieter, H. Z. E. Jaafar, S. Ercisli and M. Zia-Ul-Haq, *Bioresources*, 2015, **10**, 1434-1451.
25. T. Bhardwaj, M. Kanwar, R. Lal and A. Gupta, *Drug Dev Ind Pharm*, 2000, **26**, 1025-1038.
26. D. F. S. Petri, *Journal of Applied Polymer Science*, 2015, **132**.
27. R. C. Mundargi, S. A. Patil and T. M. Aminabhavi, *Carbohydrate Polymers*, 2007, **69**, 130-141.
28. A. Kumar, K. Singh and M. Ahuja, *Carbohydrate Polymers*, 2009, **76**, 261-267.
29. U. Mikac, A. Sepe, J. Kristl and S. Baumgartner, *J*

Control Release, 2010, **145**, 247-256.
30. T. Coviello, F. Alhaique, A. Dorigo, P. Matricardi and M. Grassi, *Eur J Pharm Biopharm*, 2007, **66**, 200-209.
31. C. Ferrero, D. Massuelle and E. Doelker, *J Control Release*, 2010, **141**, 223-233.
32. A. Bejenariu, M. Popa, D. Le Cerf and L. Picton, *Polymer Bulletin*, 2008, **61**, 631-641.
33. I. C. Alupei, M. Popa, M. Hamcerencu and M. J. M. Abadie, *European Polymer Journal*, 2002, **38**, 2313-2320.
34. A. K. Giri, *Mutation Research-Reviews in Mutation Research*, 1997, **386**, 25-38.
35. C. Mura, M. Manconi, D. Valenti, M. L. Manca, O. Diez-Sales, G. Loy and A. M. Fadda, *Carbohydrate Polymers*, 2011, **85**, 578-583.
36. K. D. Lee, S. H. Choi, D. H. Kim, H. Y. Lee and K. C. Choi, *Arch Pharm Res*, 2014, **37**, 1546-1553.
37. G. Fundueanu, M. Constantin and P. Ascenzi, *Biomaterials*, 2008, **29**, 2767-2775.
38. S. S. Sampath and D. H. Robinson, *Journal of Pharmaceutical Sciences*, 1990, **79**, 428-431.
39. L. K. Hansen, M. Brown, D. Johnson, D. F. Palme, C. Love and R. Darouiche, *Pace*, 2009, **32**, 898-907.
40. O. V. Bondar, A. V. Sagitova, Y. V. Badeev, Y. G. Shtyrlin and T. I. Abdullin, *Colloids and Surfaces B-Biointerfaces*, 2013, **109**, 204-211.
41. J. Monkare, R. A. Hakala, M. A. Vlasova, A. Huotari, M. Kilpelainen, A. Kiviniemi, V. Meretoja, K. H. Herzig, H. Korhonen, J. V. Seppala and K. Jarvinen, *J Control Release*, 2010, **146**, 349-355.
42. A. Jaipal, M. M. Pandey, A. Abhishek, S. Vinay and S. Y. Charde, *Colloids and Surfaces B-Biointerfaces*, 2013, **111**, 644-650.
43. J. L. Wang, B. C. Li, Z. J. Li, K. F. Ren, L. J. Jin, S. M. Zhang, H. Chang, Y. X. Sun and J. Ji, *Biomaterials*, 2014, **35**, 7679-7689.

The XG-SA/GS hydrogels yielded a significantly lower degree of infection than native XG-SA hydrogels in an *in vivo* rabbit subcutaneous *S. aureus* infection model at day 7.